**HEFAT2014**
**10th International Conference on Heat Transfer, Fluid Mechanics and Thermodynamics**
**14 – 26 July 2014**
**Orlando, Florida**

# A NODAL MODEL FOR SHAPE OPTIMIZATION OF OFFSET STRIP FIN HEAT EXCHANGER

Ephraïm Toubiana[1,2,3,*], Daniel Bougeard[1,2], Serge Russeil[1,2], Nicolas François[3]
1- Mines Douai, EI, F-59500 Douai, France
2- Université Lille Nord de France, F-59000 Lille, France
3- Valeo Systèmes Thermiques TPT, 8 rue L. Lormand, F-78320 La Verrière, France
*Author for correspondence
E-mail: ephraim.toubiana@mines-douai.fr

## ABSTRACT

A methodology of a nodal model implementation for heat exchanger optimization is presented as an alternative to direct CFD-based optimization. The accuracy and the interest of the use of a nodal model in the frame of optimization process for heat exchanger geometries composed of a base pattern such as offset strip fins (OSF) geometries is detailed. Then an example of optimization of OSF profiles using the nodal model and a genetic algorithm is performed.

## INTRODUCTION

Offset strip fins are widely used in heat exchangers to enhance heat transfer rate by enlarging surface area and regenerating thermal boundary layer [1] [2]. This kind of heat exchange surface has one of the highest heat transfer performances relative to the friction factor. Then it have been studied extensively both numerically [13] and experimentally. However, though many correlations are available in the literature for these types of fins, too many deviations are observed among them [14].

In order to improve heat exchangers aero-thermal performances, CFD-based optimizations can be beneficently performed [10], [12] by using adequate solvers and optimization algorithm. Though they provide very accurate results in most cases, computer power and CPU time required for those kinds of optimizations are very often too much important to supply results within a reasonable time. Moreover, during the optimization process, the absolute value of the objective function is usually not essential, but only the relative differences between compared individuals [15]. Thus, it is often not necessary to spend a large amount of computing resources to determine the exact estimate of the value of the objective functions. Instead, an approach based on inexact pre-evaluation using surrogate models can be adopted to identify the better individuals, and then perform later, only for these candidate solutions a more accurate evaluation by CFD [9][11].

## NOMENCLATURE

| | | |
|---|---|---|
| $e$ | [mm] | Fins thickness |
| $P_t$ | [mm] | Transverse fin pitch |
| $P_l$ | [mm] | Longitudinal fin pitch |
| $s$ | [mm] | Fin spacing |
| $L$ | [mm] | Longitudinal length |
| $L^+$ | [-] | Dimensionless longitudinal length for friction |
| $L^*$ | [-] | Dimensionless longitudinal length for heat transfer |
| $T$ | [K] | Temperature |
| $\Delta T_{lm}$ | [K] | Log-mean temperature difference |
| $\Delta T_{i\text{-}f}$ | [K] | $T_i$-$T_{fin}$ |
| $U$ | [m·s$^{-1}$] | Velocity |
| $I$ | [%] | Turbulence intensity |
| $D_h$ | [mm] | Hydraulic diameter ($D_h$ =2·s) |
| $\dot{m}$ | [kg/s] | Mass flow rate |
| $Re$ | [-] | Reynold number ($\rho \cdot U \cdot D_h/\mu$) |
| $Nu_L$ | [-] | Nusselt number |
| $\Delta P$ | [Pa] | Pressure drop |
| $\Delta P^*$ | [-] | Dimensionless pressure drop |
| $Nd$ | [-] | Node |
| $q''$ | [W/m$^3$] | L averaged heat flux |
| $Cp$ | [J·kg$^{-1}$·K$^{-1}$] | Specific heat at a constant pressure |
| $\lambda$ | [W·m$^{-1}$·K$^{-1}$] | Thermal conductivity |
| $\mu$ | [Pa·s] | Dynamic viscosity |
| $\rho$ | [kg·m$^{-3}$] | Density |

Subscripts

| | |
|---|---|
| *fin* | Fin |
| *i* | I-th node |
| *in* | Inlet |
| *out* | Outlet |
| *tot* | Total |
| *min* | Minimum |
| *max* | Maximum |

Therefore as a surrogate model, a nodal model has been developed to assess the aero-thermal performances of heat exchangers with several geometric characteristics. In particular, it is suited to heat exchanger geometries composed only by a base fin pattern that repeats itself along flow path such as offset strip

fin. In our nodal model approach, each occurence of the base pattern corresponds to a node. Iteratively, this correlation-based model estimates aero-thermal performance for each of these nodes in order to finally obtain the overall performance of the whole fin. Each node has not necessary the same value of some geometric parameters (such as longitudinal length) which are taken into account as correlations input. Therefore one of the interests of this particular surrogate model is that it allows us at least one degree of freedom (the variable geometrical parameter) by each node which composes the heat exchanger geometry knowing that the number of nodes that compose heat exchanger geometry is not limited. Then the number of degree of freedom (geometrical parameters) can increase strongly without require to modify the model correlations.

After the description of the nodal model and its implementation, the present paper presents, as an example of nodal model application, the optimization of two-dimensional offset strip fin heat exchanger types with a variable longitudinal fin pitch, while maintaining the same mass and volume as the reference geometry having constant transversal pitch.

## THE NODAL MODEL

A new 1D model based on correlations, themselves established by numerical simulations, has been developed to estimate the performances of heat exchanger profiles having given geometrical characteristics. In the nodal model, the heat exchanger is modeled by a set of nodes ($Nd_i$) representing each repetition of the pattern in the flow direction as presented on Figure 1.

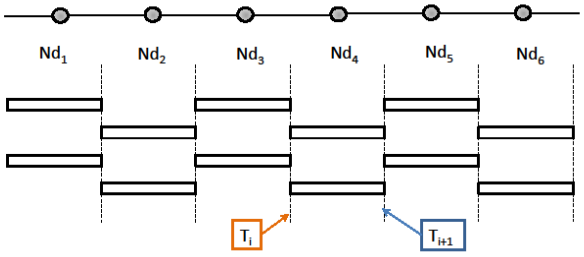


**Figure 1** Schematic illustration of the nodal model

Iteratively, the nodal model estimates the aero-thermal performance at each of these nodes to finally get the overall performance of the heat exchanger. Each node's aero-thermal performance estimation is performed by the use of CFD-based correlations to get the nodal heat transfer and pressure loss. Once the nodal model is built by the determination of the CFD-based correlations, its use in the optimization process strongly accelerates the computation time to find an optimal solution.

**Geometry**

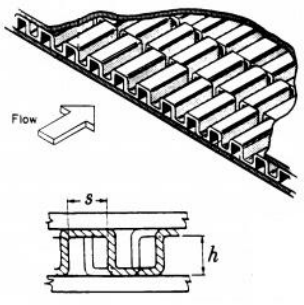


**Figure 2** Offset strip fins heat exchanger (from [2])

In this paper we develop the nodal model with the OSF fin as the base fin pattern geometry. General shape of OSF heat exchanger is illustrated in Figure 2. The reference profile used throughout this paper is a two-dimensional shape such as the one presented in Figure 3. For other OSF heat exchanger base fin pattern shapes than the two-dimensional shape used here, the method to be used is identical than presented here.

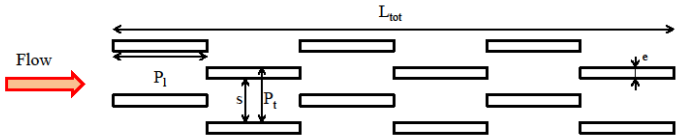


**Figure 3** Geometrical parameters

On this approach we implement correlations with a fixed transverse pitch ($P_t$) and fins thickness (e). The longitudinal fin pitch ($P_l$) can vary between $P_{l,min}$ and $P_{l,max}$. The fluid is cooled by the heat exchanger and the fins are supposed to be of fixed temperature.

The procedure to establish the nodal model has four major stages:

1- The choice of the number and the range of the nodal model's correlations parameters.
2- The achievement of CFD simulations necessary to build the correlations and results post-processing.
3- The choice of the algebraic expression of the correlations functions and identification of corresponding coefficients.
4- The validation of nodal model.

We firstly develop and explain the implementation of the nodal model, its use and limitations. Then we show its interest within the framework of an optimization shape loop.

## METHODOLOGY

### Correlations based approach

For the implementation of the nodal model, it is necessary to establish correlations. These correlations will be used afterwards by the nodal model in order to estimate for each node the value of the pressure drop and the heat exchange. These correlations are specific to each particular shape of base fin pattern. Moreover even if the geometry of the base fin pattern is identical, the correlation (or more precisely the coefficient of the algebraic function) has to be adapted if the flow and heat topology is different (not fully developed region) and of course, if the Reynolds number or the thermo physical properties of the fluid varied significantly.

For example the CFD simulation of the complete OSF heat exchanger profile shows that the first fins at the inlet (which is equivalent to the first nodes in the nodal model) of the heat exchanger and the last fin at the output inlet (which is equivalent to the last node in the nodal model) do not have a similar flow structure as internal flow exchanger fins. This edge effect is taken into account in our procedure by establishing specific correlations for the first and the last node of the profile. Therefore our approach will take into account the effects of establishment in the inlet and outlet.

So we establish three kinds of correlations: one for the first node (Cor1), one for the last node (CorN) and one for all internal nodes (CorI).

To do this, we based the functional form of our correlations on the correlations developed by Stephan (1959) [5] for heat exchange ($Nu_L$) , and Shah and London (1978) [6] for viscous losses ($\Delta P^*$) in laminar developing flow of a 2D duct. These new correlation are dependent on the dimensionless longitudinal length of the fin.

Thus for overall Nusselt number $Nu_L$ for one fin (which will correspond to one node on the nodal model), the functional form correlations is written as follow:

$$Nu_L = A_1 + \frac{B_1 \cdot (L^*)^{C_1}}{1 + D_1 \cdot (L^*)^{E_1}}$$

With $L^* = \frac{L}{D_h \cdot Re \cdot Pr}$ , $Nu_L = \frac{q" \cdot D_h}{\Delta T_{lm} \cdot \lambda}$ and $\Delta T_{lm} = \frac{(T_i - T_{fin}) - (T_{i+1} - T_{fin})}{\ln(T_i - T_{fin})/(T_{i+1} - T_{fin})}$

Similarly, it is assumed that the functional form of dimensionless pressure drop $\Delta P^*$ is:

$$\Delta P^* = A_2 \cdot \sqrt{L^+} + \frac{B_2 \cdot L^+ + C_2 - D_2 \cdot \sqrt{L^+}}{1 + E_2 \cdot (L^+)^{-2}}$$

With $L^+ = \frac{L}{D_h \cdot Re}$.

Then to determine all of the parameters needed for the three correlations (Cor1 CorI and CorN) for $Nu_L$ and $\Delta P^*$ we perform a set of CFD simulations.

Besides, as will be detailed in the next paragraph, the computational domain to establish Cor1 and CorN (for first and last node) is not the same as that used to establish CorI for internal nodes (See Figures 4 and 5).

### CFD simulations

The entire CFD simulations where carried out using the commercial code Starccm+ 8.04.

Steady simulations where performed with a RANS approach and the k-ϵ realizable turbulence model with two-layer approach near walls [16] has been used.

In this model it is assumed that:

- The flow is incompressible
- The fluid is the air and thermo-physical properties constant except for ρ
- Natural convection and radiation are neglected

As mentioned this model will take into account the effects of establishment in the inlet and outlet (Figure 5). To establish the internal correlations (CorI) the computational domain (D1) is limited to one base pattern (see Figure 4).

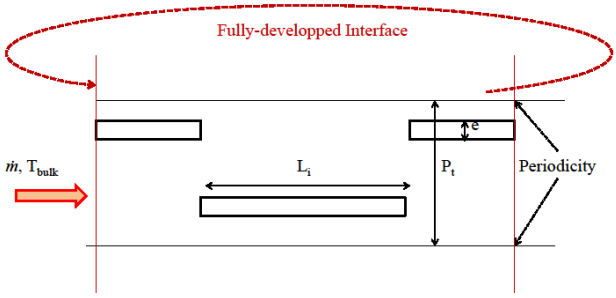


**Figure 4** D1 and operating conditions

To establish the correlations Cor1 and CorN, the computational domain (D2) and the boundary conditions are described in figure 5 It has to be noted that the number of internal fins in each CFD simulation is variable and depends mainly on the longitudinal length of the fins in order that total length will be large enough so that there is no interference between inlet effects and outlet effects.

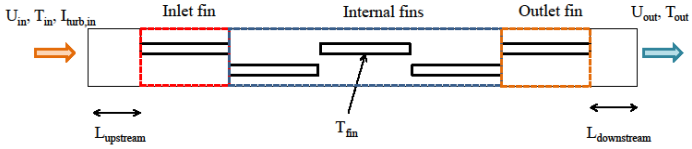


**Figure 5** D2 and operating conditions

To establish the correlations two kinds of simulations are performed: for $Nu_L$ anisothermal simulations are performed, while to determine $\Delta P^*$ isothermal simulations are performed.
The fins are assumed to be of constant temperature which is fixed for the establishment of the correlations $T_{fin}$=333K, and the fluid is warmer than fin (the fluid is cooled).
Moreover, the following settings are generally used in the calculations made on complete profiles (Figure 5) :
At the inlet, a uniform velocity is imposed with turbulent intensity of 7 %, the turbulence length scale is considered equal to 7% of the inlet hydraulic diameter.
Two additional regions are added upstream and downstream. One on the inlet region, following the inlet velocity condition, for the flow development with $L_{upstream} = 12 \cdot D_h$. And the other on the outlet region preceding the outlet pressure condition for flow tranquillizing with $L_{downstream} = 35 \cdot D_h$
When isothermal calculations are performed we take for internal nodes $T_{iso}$=333.15K, and for first and last nodes $T_{iso}$=483.15K (The Reynolds number is constant for any simulation).
A grid sensitivity analysis has been performed which shown that hexahedral mesh is more adapted to our study. For that, about twenty schemes including the use of polyhedral mesh and an increasing number of cells with refinement on the walls.
We verified that the pressure drops and heat exchanged become insensitive to the resolution of the mesh. Moreover we ensure that the value of the non-dimensional wall $y^+$ was close to unity.
Once the CFD simulations performed, in order to determine the correlation function of $Nu_L$ and $\Delta P^*$, for each function we define $E_c$ as the sum of squared relative residuals and we look for the coefficients value which minimize $E_c$ (least squares method). The results are presented on Figure 6 and Figure 7.

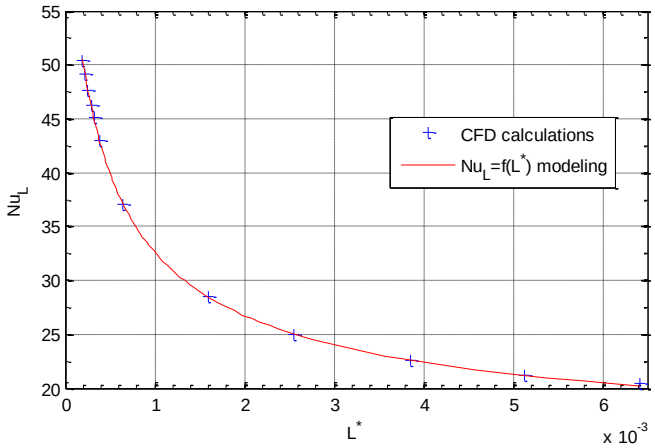


**Figure 6** $Nu_L$ correlations and CFD Points

With the coefficients chosen in this way, the largest relative deviation over the 13 points calculated by CFD is 0.94% for $Nu_L$ and 1.00% for $\Delta P^*$. However the mean relative deviation over the 13 points calculated by CFD is only 0.08% for $Nu_L$ and 0.07% for $\Delta P^*$.

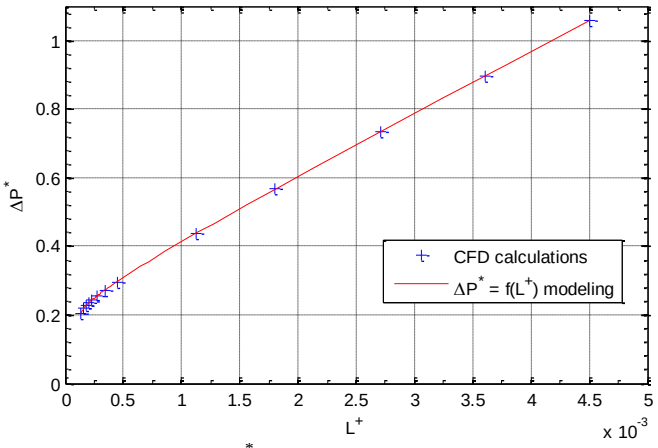


**Figure 7** $\Delta P^*$ correlations and CFD points

**Influence of the flow temperature on correlations**

CFD simulations to establish correlations were performed with conditions of fixed temperature. But some CFD simulations have shown that it is necessary to take into account the impact of the temperature difference between the walls and the fluid to be more accurate. As shown in figure 8, for $L^*$ fixed, if $\Delta T_{i-f}$>5K, $Nu_L$ varies linearly with $\Delta T_{i-f}$.
More generally, it is possible to model $Nu_L = f(\Delta T_{i-f})$ for $L^*$ fixed, as follows :

$$Nu_L(\Delta T_{i-f}) = A(L^*) \cdot \Delta T_{i-f} + B(L^*)$$

With A and B functions of $L^*$.
There is thus:

$$Nu_L(T_{in} - T_{wall}) - Nu_L(350 - T_{wall}) = A(L^*) \cdot [(T_{in} - T_{wall}) - (350 - T_{wall})] + B(L^*) - B(L^*) = A(L^*) \cdot (T_{in} - 350)$$

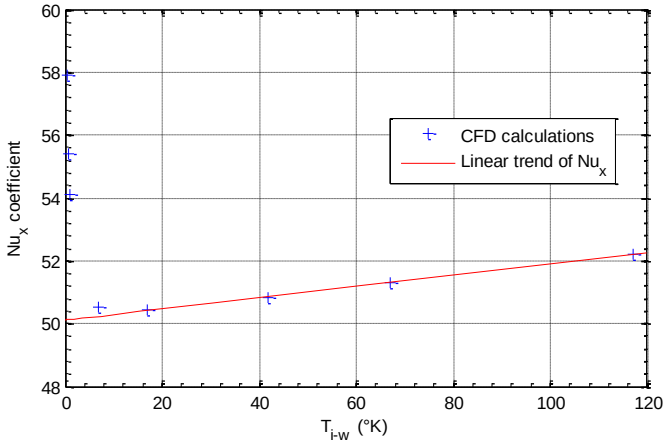


**Figure 8** Linear hypothesis of $Nu_L$ variation for $L^*=0.92 \cdot 10^{-4}$

This allows us to have a direct relationship between the value of $Nu_L$ for any value of $T_{in}$ and the value of $Nu_L$ established for $T_{in}$= 350K (within the range of validity of the linear assumption for $Nu_L(\Delta T_{i-f})$ )

$$Nu_L(\Delta T_{i-f}) = Nu_L(\Delta T_{350}) + A(x^*) \cdot (T_{in} - 350)$$

With $\Delta T_{350}$=350K-333K which is the $\Delta T_{i-f}$ used to establish the correlations.
The next step is to determine the function $A(L^*)$.
In Figure 9 it can be observed that we can model $A(L^*)$ by a power function. Thus we have the modelling function of $Nu_L(\Delta T_{i-f})$:

$$Nu_L(\Delta T_{i-f}) = Nu_L(\Delta T_{350}) + (a.L^{*b} + c)\,(L^*) \cdot (T_{in} - 350)$$

With a, b and c constants that depend only on the transverse pitch $P_t$ which is constant here.

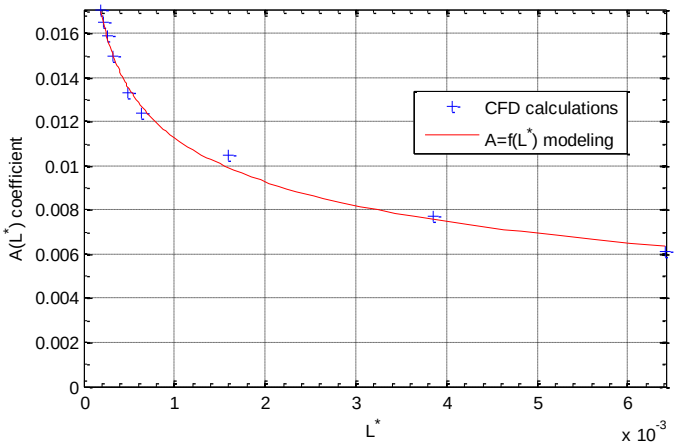


**Figure 9** A($L^*$) coefficient regression

**Establishment effects**

We investigated through a series of simulations (CFD) the nature and impact of the establishment effects on the reference Reynolds number. To take into account those effects in the nodal model, correlations are established for the first and last fin profile with a functional form similar to internal fins correlations. The CFD simulations have shown that the establishment effect last on the same longitudinal length whatever is the longitudinal length of the first fin. So if the longitudinal length of the first fin is very short it is possible that the input establishment effect will last over more than the first fin (which is the first node of the model). Therefore the higher is the input fin long, the more the input establishment effects are fully taken into account by our approach and then the more the nodal model is accurate. However we found that the output establishment effects are limited to the last fin even if the last fin is very short $L_N=L_{i,min}$. On Figure 10 it is presented a comparison between CFD and the nodal model of the ΔP caused by each node that compose a profile with constant $L_i=L_{i,min}$ on isothermal flows. We can observe on this figure the difference on nodal model estimation when it takes into account the establishment effect or not. The impact of establishment effect with $L_1=L_i=L_{i,min}$ last over about the first 5mm in the inlet region. The case presented is the more unfavourable case, but generally $L_1 > L_{i,min}$ so the input establishment effect last only on the first or the two first nodes. However even for $L_i=L_{i,min}$, on the outlet region those effect are predominately only on the last fin.

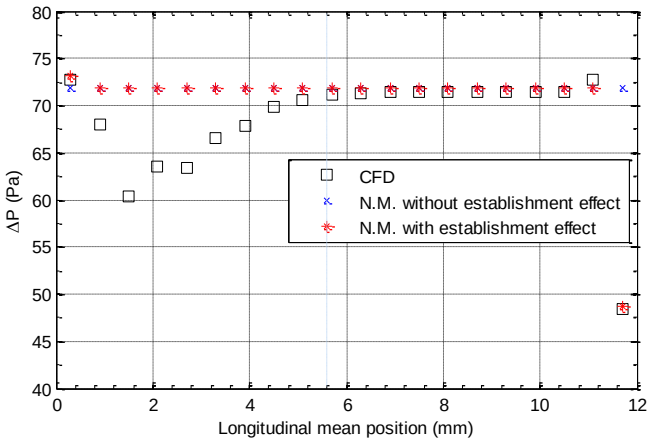


**Figure 10** Impact of establishment effects on isothermal flows with $L_i=L_{i,min}$

**Iterative calculation of the distribution of the fluid's nodal temperature and pressure drop**

In the preceding paragraphs, the methodology for determining the correlations is presented. Now we present how we are implementing the nodal model. For this, we proceed in two steps. First of all fluid temperature (i.e. heat transfer) is calculated iteratively for each node of the heat exchanger (See Figure 11) and only then the calculation of the pressure drop at each node is performed (See Figure 12).

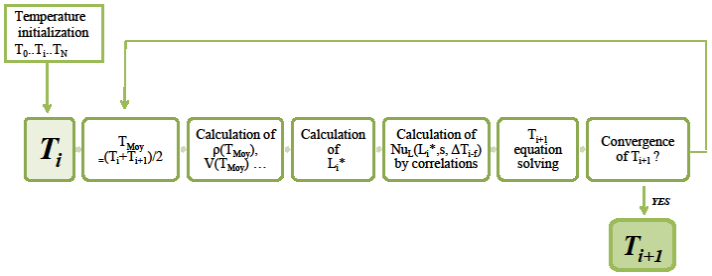


**Figure 11** Iterative calculation of the temperature at each node

As illustrated in Figure 11 the calculation of the distribution of the fluid's nodal temperature is done in an iterative way. This means that it is necessary to know the temperature of the fluid at the previous node to determine the temperature of the fluid next node.

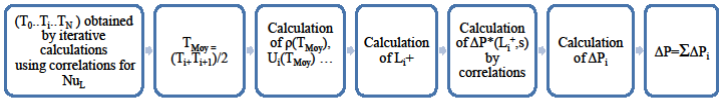


**Figure 12** Procedure of calculation of the pressure drop

At each node the temperature calculation is done in the following way for our OSF geometry.

We have:

$$Nu_L = \frac{q'' \cdot D_h}{\Delta_{lm} \cdot \lambda}$$

In addition, following the first law of thermodynamics we have for one node (i.e. fin) of longitudinal length $L_i$ with $T_i$ the input temperature of the node, $T_{i+1}$ the output temperature of the node and $S_{fin}$ the fin surface:

$$q" \cdot S_{fin} = \dot{m} \cdot C_p \cdot (T_{i+1} - T_i)$$

After calculations we get:

$$q" = \frac{\rho \cdot U_i \cdot s \cdot C_p \cdot (T_{i+1} - T_i)}{2 \cdot (L_i + e)}.$$

Then:

$$Nu_L = \frac{\rho \cdot U_i \cdot s^2 \cdot C_p \cdot \ln \frac{T_{fin} - T_i}{T_{fin} - T_{i+1}}}{\lambda \cdot (L_i + e)}.$$

Therefore we get:

$$T_{i+1} = T_{fin} - \frac{T_{fin} - T_i}{\exp \frac{Nu_L(L^*) \cdot \lambda \cdot (L_i + e)}{\rho \cdot U_i \cdot s^2 \cdot C_p}}.$$

Where $Nu_L$ is determined by the established correlations.
Thus in an iterative way we solve the outlet temperature of each node ($T_{i+1}$) which is the inlet temperature of the next node. Moreover, if the thermo-physical properties are assumed to vary with temperature, it is necessary to calculate their value at each node taking the mean value of the temperature of the node $T_{moy}=(T_i+T_{i+1})/2$. Furthermore because of the implicit definition of $T_{moy}$, at each node, there is also an iterative calculation until convergence of $T_{i+1}$ as illustrated in Figure 11.
Once the nodal temperature distribution of the fluid is completely determined, we can calculate the pressure drop via the nodal correlations $\Delta P^*(x^+)$. Indeed, knowing the temperature of the fluid at each node, it can easily determine the nodal values of $L^+$, $U_i$ and ρ.
Thus, for each node we have:

$$\Delta P_i = \Delta P_i^*(L^+) \cdot \frac{\rho \cdot U^2}{2}$$

Then to calculate the total pressure drop of the profile we have:

$$\Delta P = \sum_i \Delta P_i$$

This approach is summarized in Figure 12.

## VALIDATION OF THE NODAL MODEL

To validate the nodal model several types of comparison with CFD were established.
First of all, a comparative between the CFD and the nodal model was performed on a specific OSF profile with variable fin length along flow path of heat exchanger i.e. having the value of successive longitudinal length different. Those comparisons where conducted both at global level and at local level, i.e. fin by fin. So in this step we will use OSF geometries with increasing or decreasing successive longitudinal length ($L_i$). To that we define 7 cases.

| Case | Growth of $L_i$ | Observations |
|---|---|---|
| $C_1$ | Strongly decrease | $L_1=L_{min}$ |
| $C_2$ | Decrease | |
| $C_3$ | Weakly decrease | |
| $C_4$ | - | $L_i$ constant |
| $C_5$ | Weakly increase | |
| $C_6$ | Increase | |
| $C_7$ | Strongly increase | $L_{15}=L_{min}$ |

For all of those case $T_{in}$=483.15, $T_{fin}$=333.15 and the heat exchangers are composed by 15 nodes (or base pattern).

**Comparison of aero-thermal performance at a local level**
We present at Figure 13 and 14 the comparison of the evolution of heat exchange and pressure drop fin by fin for cases $C_1$ and $C_7$ at a local level i.e. node by node. On the following figures (13 and 14) each points represent a node (and so the local value of pressure drop and temperature). For the CFD results the values of ΔP of each fin (or node) that compose the profile is calculated from the longitudinal force applied on each fins. Similarly the temperature is calculated from the heat exchange on each fin. The curves show the variation along flow path of longitudinal length.

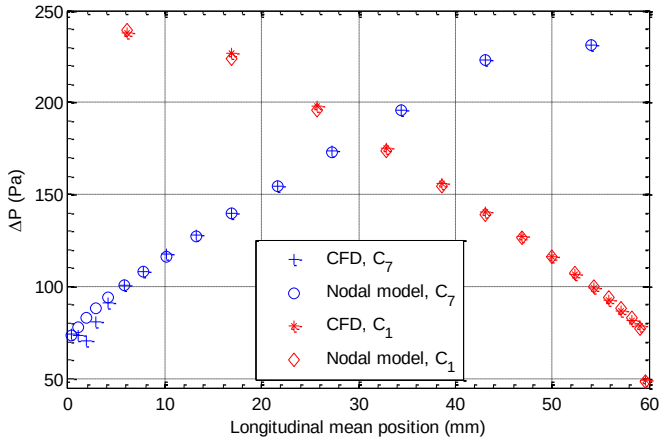


**Figure 13** Comparison between the nodal model and CFD on isothermal flows at local level

In those figures we can see for each case (C1 and C7) the closeness of the two curves the one corresponding to CFD calculation and the other one to the calculation with the nodal model.

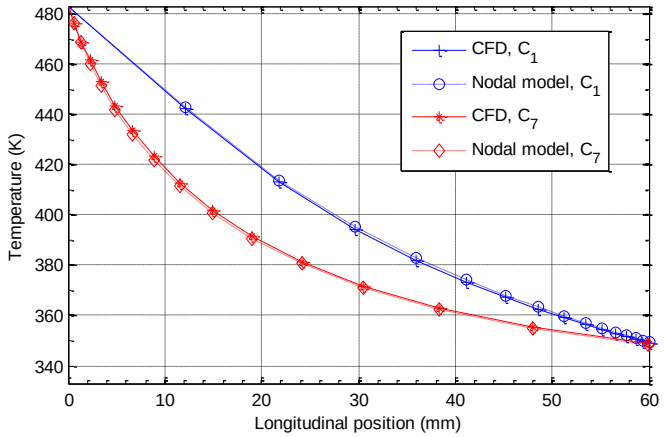


**Figure 14** Comparison between the nodal model and CFD at local level

It was also analyzed the impact of taking into account the variation of $Nu_L$ with $\Delta T_{i-f}$ and was noticed the importance of corrective factor on the accuracy of calculation (on the order of 1-2% on $Nu_L$).

### Comparison of aero-thermal performance at a global level

In this section we make a comparison between the overall aero-thermal performance provided by the CFD and those provided by the nodal mode.
We can see in Figure 15 the comparison between the nodal model and CFD for outlet temperature ($T_{in}$=483.15K). For all the cases presented here, the relative difference between the nodal model and CFD on overall Nusselt number is of the order of 1%. On Figure 16 we performed the same kind of comparison but on isothermal flows for the pressure drop. As for heat exchange, we observed that the nodal model is very accurate with a difference between the nodal model and CFD on ΔP of the order of 1%

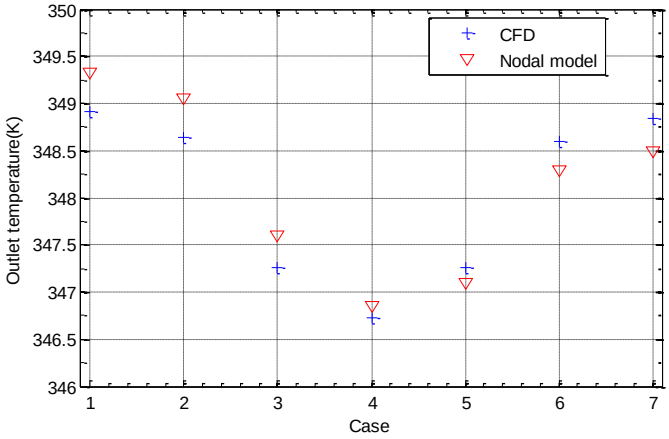


**Figure 15** Comparison between the nodal model and CFD for outlet temperature

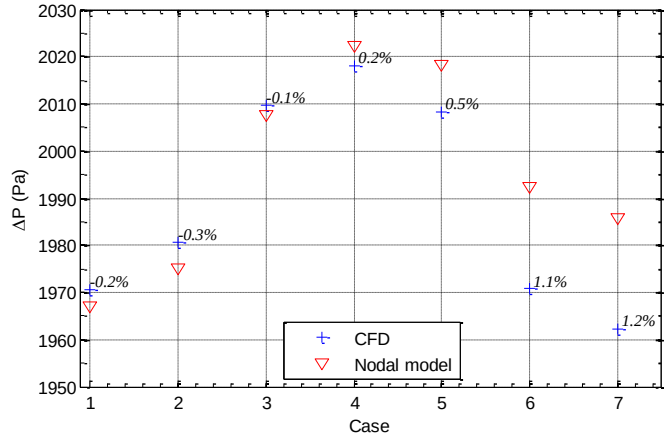


**Figure 16** Comparison between the nodal model and CFD for isothermal flows with relative difference (%)

### Accuracy and limits

We have seen in several calculations through comparison between the nodal model and CFD that the nodal model has good accuracy: generally <3% on absolute pressure drop (see e.g. Figure 16) and on $Nu_L$. Among the factors that have a significant impact on the accuracy of nodal model may be mentioned the total length $L_{tot}$ of the profile and the length of the input fin $L_1$. In fact, the more $L_{tot}$ is long, the greater the establishment effects on the profile entry are negligible. Similarly, the more $L_1$ is long, the better the establishment effects will be considered, as the impact of this effect on the following fins will be less significant (which not taken into account in the nodal model).
Regarding the number of CFD simulation used to build the nodal model, it was perfomed about sixty calculations knowing that most of the calculations (85%) are performed on a bi-periodic pattern composed of only two fins (Figure 4). The required CPU time to this number of simulation is quite low when compared to the required CPU time for numerical simulation of complete profiles.

## OPTIMIZATION OF VARIABLE LONGITUDINAL LENGTH OF OSF PROFILES BY THE NODAL MODEL

One of the interests of this nodal model is that we can estimate aero-thermal performances of thousands of OSF geometric configurations extremely quickly. Can be varied for example, the total length, the number of fins (i.e nodes), the length of each fin (which can be different from one to other) etc. That allows us to achieve multi-objective optimization, or simply response surface, by means of a platform enabling an automatic optimization process such as Isight software. The general scheme of the optimization process is illustrated on Figure 17

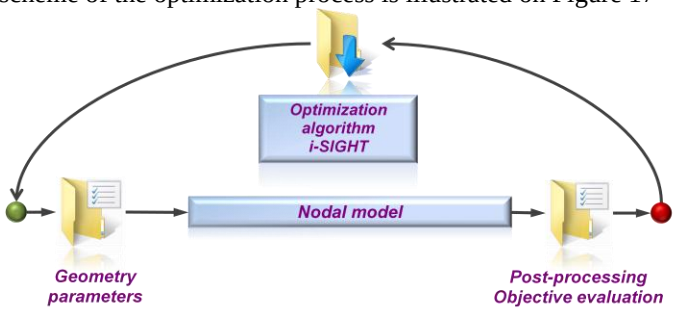


**Figure 17** Optimization process

### Multi-objective optimization

The objectives of an optimization process are often conflicting with each other: an increase of one objective such as pressure drop will lead to the decrease of the other objective such as heat exchange. There is no best solution for which all objectives are optimal simultaneously. Then such challenges can be answered thanks to multi-objective optimization. The multi-objective optimization means that we would like to simultaneously improve the values of all objectives, while complying with some additional constraints as well.
The optimization problem can be formulated as

$$\min_{x \in \mathbb{R}^n} (f_1(x), f_2(x), \dots, f_m(x))$$

$$\text{Subject to } \begin{cases} g_k(x) \le 0, \ \forall k = 1,2,\dots,K \\ g_l(x) = 0, \ \forall l = 1,2,\dots,L \end{cases}$$

Where x is the vector of design variables, $f_1(x)$, $f_2(x)$,..,$f_m(x)$ are the m objective functions, and $g_k(x)$, $g_l(x)$ are the inequality and equality constraints, respectively. According to constraints, $x \in X \in \mathbb{R}^n$ must be satisfied, where X is the set of feasible

designs. Then, we have to be a set of solutions, the so-called Pareto optimal set or Pareto front, in which one solution cannot be dominated by any other member of this set. To perform the profile geometry optimization we choose as optimization algorithm the non-dominated sorting genetic algorithm II (NSGA-II) proposed by Deb et al. [7] witch is one of the most widely used multi-objective genetic algorithms (MOGA).

In order to improve the heat exchangers aero-thermal performances several kinds of optimizations could be performed such as CFD-based optimizations. Nevertheless computer power and CPU time required for those kinds of optimizations are very often too much important to supply results within a reasonable time. The time saving by the use the nodal modal is of the order of a ratio of $10^4$ at least compared to classical CFD based optimization. As an indication for one CFD simulation of a heat exchanger with the same conditions as to establish the correlations with $L_{tot}$=60mm we need a CPU time on the orther of 100 hours, on the other hand the nodal model provides us an estimation of the order of 10-20 different geometrical configurations in only 1 second.

The use of the nodal model as a surrogate model allows us to perform optimization with a high number of parameters defining the profile geometry without an excessive loss of the accuracy of the performance estimation.

As an illustration of the optimization possibilities that allows us the nodal model, we will perform in the following paragraph an optimization of OSF profiles with variable fin length by the nodal model. Our objective is not to enter in the details of the parameters used in this optimization used but only to illustrate the interest of using the nodal model as a surrogate model.

In the following paragraphs we will use:

| *Constant parameter* | *Value* |
|---|---|
| $T_{in}$ | 483.15 K |
| $T_{fin}$ | 333.15 K |
| $L_{tot}$ | 60 mm |
| N | 15 fins |

**Optimization of OSF geometries with variable fin length along flow path**

The interest to perform an optimization process of OSF heat exchangers geometries with variable fin length along flow path is due to some considerations. Firstly, when the flow is passing through an OSF profile, the fluid physical properties, such as its speed, its temperature, varies according to its longitudinal position. On the other hand, the lower is the difference between the fluid and the fins temperature, the lower is the heat exchange between the fluid and the air and thus the fluid temperature less varies longitudinally. Therefore, one of the fundamental questions that arise regarding the OSF profile is whether an ideal profile would be precisely a profile whose successive fins have different longitudinal length depending on the longitudinal position of the fin, i.e. depending on the intensity of the variation of the fluid temperature.

Moreover for louvered fins heat exchanger, Hsieh and Jang[4] proposed successively increased or decreased louver angle patterns and they carried out a numerical analysis on heat and fluid flow. Their results indicated that successively variable louver angle patterns applied in heat exchangers could effectively enhance the heat transfer performance. So to provide first answers to this question we have implement a series of optimization loop. We will attempt to understand in which cases this kind of profile is of interest, if the advantage of this type of profile is significant enough etc.

Then we perform an optimization loop using several parameters which determines the successive longitudinal length ($L_i$) of the nodes. To be note that to each compared heat exchanger geometry, the successive node's longitudinal length growth (increase or decrease) is monotonically

About 5000 individuals (which are each one a geometric configuration) have been estimated by the nodal models within about five minutes only.

The Pareto front (non dominated points) is presented in Figure 18.

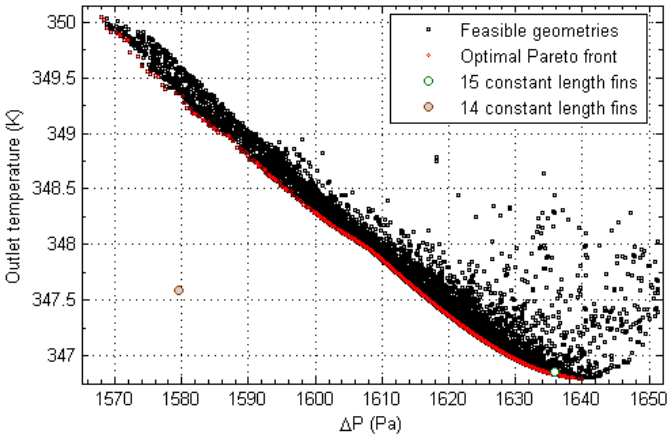


**Figure 18** Optimization results

First of all, to be note that almost each of optimal geometries have longitudinally decreasing length ($L_{i+1} < L_i$).

We can also observe that the benefits of OSF geometries with variable fin length along flow path in comparison with constant length fin profiles are not significant or measurable. In fact the reference profile of 15 constant length fin OSF profile belongs to the Pareto front. Therefore it will be of interest to perform wider optimization loop with variable fins number. Moreover it perhaps not impossible that with other flow conditions such as laminar or very turbulent flow or with greater temperature gap ($\Delta T_{i-f}$) between the flow and the fins or even with other shape of the base pattern, this result would be different. Moreover some CFD simulations have been performed for several individuals belonging to the Pareto front and others which not belong to Pareto front, in order to validate this nodal based optimization. It was confirmed that the individuals who belonged to the Pareto front by this optimization remain optimal on CFD simulations when they are compared with the individuals who not belong to Pareto front.

## TO GO FURTHER WITH NODAL MODEL

Several areas for improvement or generalization of the nodal model are possible and have an interest in the framework of optimization.
First of all, take into account of the possible variation of the transverse pitch ($P_t$). New correlations are currently developed with a slight different method and without taking into account the establishment effects. That allows us to perform other kind of optimizations and to analyze for example the impact of several constraints such as constant mass, constant longitudinal length etc. on optimal design. However due to length restrictions the descriptions of generalized nodal model fall beyond the scope of this paper.
Another improvement possible is to take into account a variation of Reynolds number. This will allow us to perform optimizations loop without constraint on Re number. Then we could for a example vary $U_{in}$ in order to have constant pressure drop or constant ventilation power between each compared geometry on the optimization process.

Finally, this model could easily generalized to other shapes of the base patterns of OSF profiles, or even other types of profiles composed by a base pattern such as weavy fins (to optimize heat exchanger geometries with non constant wavelength for example).

## CONCLUSION

In this paper it was presented the development of a nodal model allowing us to evaluate nodal aero-thermal performance of heat exchangers made from a fin base pattern that longitudinally repeats itself as the OSF heat exchangers. In this iterative approach, each instance of the base pattern corresponded to a node and the aero-thermal performances evaluation of this node is based on correlations determined by CFD. It was presented the methodology of modeling these correlations that depends on the parameters that are to be taken into account in the nodal model, such as the impact of establishment effects, the impact of temperature on some coefficients etc. Among the variables parameters taken into account by the nodal model include the total length of the profile, the number of fins component profile, choosing the length of each fin (not necessarily identical).
Some optimizations of OSF geometries with variable fin length along flow path by the nodal model have been performed by the use of the nodal model using sequences defining successive longitudinal length. It has been observed that for the flow conditions used, the geometries with longitudinally increasing fin length are generally not optimal. Moreover geometries with constant length fins belong to the Pareto optimal front even when fin numbers are variables. So for the used flow conditions and this specific OSF base pattern shape, OSF geometries profiles with variable fin length along flow path have not significant gain.
Finally due to his accuracy level, the nodal model can also be used as a tool for a fast sizing of heat exchangers by the use of only few small CFD simulations.

## REFERENCES


[1] R.K. Shah and D.P. Sekulic. Fundamentals of Heat Exchanger Design. Wiley, 2003
[2] R.M. Manglik, A.E. Bergles, Heat transfer and pressure drop correlations for rectangular offset stripfin compact heat exchanger, *Experimental Thermal and Fluid Science* 10 (1995) 171-180
[3] Thévenin D, Janiga G. Optimization and computational fluid dynamics. 1st ed. Springer-Verlag Berlin Heidelberg; 2008.
[4] C.T. Hsieh, J.Y. Jang, 3-D thermal-hydraulic analysis for louver fin heat exchangers with variable louver angle, *Applied Thermal Engineering* 26 (2006) 1629-1639.
[5] Stephan K., 1959, Warmeubergang und drauckabfall bei nicht ausgebildeter Laminarstromung in Rohren undin ebenen Spalten, Chem.-Ing.-Tech.,Vol 31, p. 773-778
[6] R.K. Shah and A.L. London. Laminar flow forced convection in ducts : a source book for compact heat exchanger analytical data. *Advances in Heat Transfer : Supplement*. Academic Press, 1978
[7] K. Deb, A. Pratap, S. Agarwal, T. Meyarivan, A fast and elitist multiobjective genetic algorithm: NSGA-II, *IEEE Transaction Evolutionary Computation* 6 (2002) 182–197
[8] Y.S. Muzychka, M.M. Yovanovich, Pressure drop in laminar developing flow in noncircular ducts: a scaling and modelling approach, *J. Fluids Eng*. 131 (2009) 111105 (11 p.).
[9] K. Saleh, O. Abdelaziz, V. Aute, R. Radermacher, S. Azarm, Approximation assisted optimization of headers for new generation of air-cooled heat ex-changers, *Appl. Therm. Eng.* (2012).
[10] Wang, Y., He, Y.L., Mei, D.H., Tao, W.Q., 2011. Optimization design of slotted fin by numerical simulation coupled with genetic algorithm. *Appl. Energy* 88 (12),4441–4450.
[11] Yue-Tzu Yang, Shih-Chia Lin, Yi-Hsien Wang, Jen-Chi Hsu, Numerical simulation and optimization of impingement cooling for rotating and stationary pin–fin heat sinks, *International Journal of Heat and Fluid Flow*, Volume 44, December 2013, Pages 383-393
[12] László Daróczy, Gábor Janiga, Dominique Thévenin, Systematic analysis of the heat exchanger arrangement problem using multi-objective genetic optimization, *Energy*, Volume 65, 1 February 2014, Pages 364-373
[13] Selma Ben Saad, Patrice Clément, Jean-François Fourmigué, Caroline Gentric, Jean-Pierre Leclerc, Single phase pressure drop and two-phase distribution in an offset strip fin compact heat exchanger, *Applied Thermal Engineering*, Volume 49, 31 December 2012, Pages 99-105
[14] L. Sheik Ismail, R. Velraj, C. Ranganayakulu, Studies on pumping power in terms of pressure drop and heat transfer characteristics of compact plate-fin heat exchangers—A review, *Renewable and Sustainable Energy Reviews*, Volume 14, Issue 1, January 2010, Pages 478-48
[15] S. Vakili, M.S. Gadala, Low cost surrogate model based evolutionary optimization solvers for inverse heat conduction problem, *International Journal of Heat and Mass Transfer*, Volume 56, Issues 1–2, 1 January 2013, Pages 263-273
[16] CD-adapco 2013. STAR-CCM+ Version 8.06 User Guide.